National Oceanography Centre

NATURAL ENVIRONMENT RESEARCH COUNCIL

National Oceanography Centre

Internal Document No. 06

On the impact of a radiational open boundary condition on continental shelf resonances

D J Webb

2013

National Oceanography Centre, Southampton
University of Southampton Waterfront Campus
European Way
Southampton
Hants SO14 3ZH
UK

Author contact details
Tel: +44 (0)23 8059 6199
Email: djw@soton.ac.uk

© National Oceanography Centre, 2013

DOCUMENT DATA SHEET

AUTHOR WEBB, D J	*PUBLICATION DATE* 2013

TITLE

On the impact of a radiational open boundary condition on continental shelf resonances.

REFERENCE

Southampton, UK: National Oceanography Centre, Southampton, 7pp.
(National Oceanography Centre Internal Document, No. 06)
(Unpublished manuscript)

ABSTRACT

Studies carried out with a one-dimensional model of a continental shelf and deep ocean have shown that the use of a radiational boundary condition doubles the decay rate of the shelf resonances. This note reports on a study using a model of the English Channel and Irish Sea which shows that, in this more realistic model, a radiational boundary condition based on Flather (1976) has a much smaller effect.

KEYWORDS

ISSUING ORGANISATION

National Oceanography Centre
University of Southampton Waterfront Campus
European Way
Southampton SO14 3ZH
UK

Not generally distributed - please refer to author

On the Impact of a Radiational Open Boundary Condition on Continental Shelf Resonances

David J. Webb

National Oceanography Centre, Southampton SO14 3ZH, U.K.

Abstract.
Studies carried out with a one-dimensional model of a continental shelf and deep ocean have shown that the use of a radiational boundary condition doubles the decay rate of the shelf resonances. This note reports on a study using a model of the English Channel and Irish Sea which shows that, in this more realistic model, a radiational boundary condition based on Flather (1976) has a much smaller effect.

1 Introduction

Webb (2013) investigated the resonances of the English Channel and Irish Sea and showed that the high tides of the Bristol Channel and Gulf of St. Malo were primarily caused by two quarter-wavelength resonances trapped between the continental shelf edge and the coastline. The first of these had a maximum at the head of the Bristol Channel and a small effect in the Gulf of St Malo. It complex angular velocity was $13.14 - i1.63\ \mathrm{rad/day}$, the real component giving the rate of oscillation and the negative of the imaginary component giving the rate of decay. The second resonances, at a complex angular velocity of $14.66 - i2.08\ \mathrm{rad/day}$ had large amplitudes in both the Bristol Channel and the Gulf of St Malo.

The earlier study was carried out using a numerical model with Dirichlet open boundary conditions. As a result each resonance had zero amplitude on the open boundary. This meant that they could not radiate energy into the deep ocean and so their decay was due solely to energy loss on the shelf. In reality such resonances can radiate energy into the deep ocean and a study of one-dimensional system (Webb, 2011) has shown that this may double the decay rate of the resonance.

This may have practical consequences. For example if a tidal barrage were built in the Bristol Channel it would change the natural frequency of the resonance and so may affect the tidal height in the region. However a resonance with a large decay rate would be much less affected by such changes than one with a small decay rate.

The present study investigates the effect of a radiational boundary condition on realistic resonances by developing the scheme proposed by Flather (1976). It does this by changing the open boundary condition so that it represents a defined incoming wave plus an outgoing wave whose complex amplitude is known only after the full model solution has been calculated. Both waves at the open boundary are assumed to be long gravity waves with a phase velocity at right angles to the boundary.

Section 2 of the paper is concerned with the details of the boundary condition used. This is used in section 3 to recalculate the complex response function of the shelf region and to investigate any changes in the position and spacial structure of the major resonances. The results show that radiation of energy into the deep ocean has only a small effect on continental shelf resonances.

2 The Open Boundary Condition

The model used for the present study is based on that described by Webb (2013). This solved a linear form of Laplace's tidal equations at a single angular velocity using an Arakawa-C grid. At the open boundary the original model used Dirichlet boundary conditions in which the tidal height ζ_b was fixed.

For the present study the model has been modified to allow radiation of energy back into the deep ocean. When using a time dependent model, Flather (1976) did this using a simple gravity wave scheme in which the normal velocity on the boundary is given by,

$$u = u_i + (\zeta - \zeta_i)c/h. \tag{1}$$

Correspondence to: D.J.Webb (djw@soton.ac.uk)

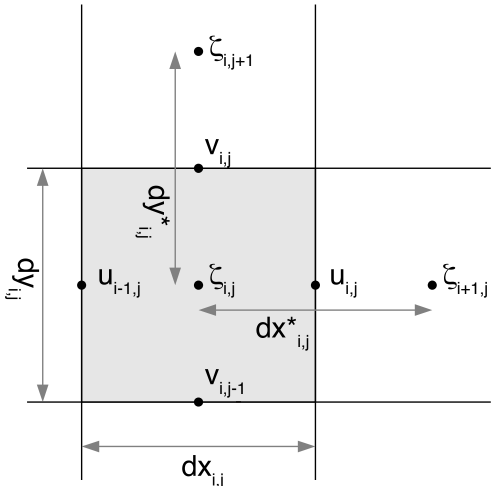

Fig. 1. The Arakawa-C Grid, showing the relative position of sea level grid points (ζ) and the easterly (u) and northerly (v) components of velocity. The shaded are is the 'grid cell' surrounding the point $\zeta_{i.j}$. The distances $dx_{i,j}$, $dy_{i,j}$, $dx^*_{i,j}$ and $dy^*_{i,j}$ refer to the grid spacing along the boundaries of each grid box and between box centres.

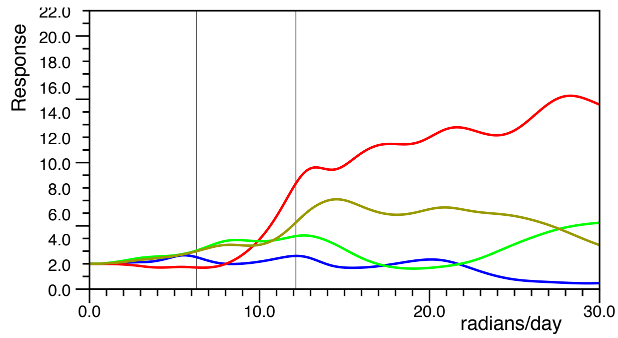

Fig. 2. The response function amplitude as a function of angular velocity for Portishead (red), St Malo (brown), Workington (blue) and Le Havre (green). Vertical lines indicate the angular velocities of the K1 and M2 tides.

where ζ and u are sea level and velocity normal to the boundary, ζ_i and u_i are the corresponding values for the incoming forced wave, h is depth and, if g is gravity, c the wave speed, equals $(gh)^{1/2}$.

For a single angular velocity ω, this is equivalent to representing the solution at the open boundary as the sum of incoming and outgoing waves propagating normal to the boundary,

$$\begin{aligned} \zeta &= (A\exp(ikx) + B\exp(-ikx))exp(-i\omega t)\,, \\ u &= (A\exp(ikx) - B\exp(-ikx))(c/h)exp(-i\omega t)\,. \end{aligned} \tag{2}$$

where A and B are the amplitudes of the incident and reflected waves, x is the coordinate normal to the boundary and k, the wavenumber in deep water, equals ω/c.

In terms of the Arakawa-C grid (see Fig. 1), consider the case where $\zeta_{i,j}$ lies on the open boundary at the point where x equals zero. Assume also that $u_{i,j}$ lies in the positive x direction and is within the model domain. If the grid spacing in the x direction is δx then,

$$\begin{aligned} \zeta_{i,j} &= (A+B)exp(-i\omega t)\,, \\ u_{i,j} &= (A\Delta - B\Delta^{-1})(c/h)exp(-i\omega t)\,. \end{aligned} \tag{3}$$

where Δ equals $\exp(i\omega\delta x/(2c))$. After eliminating B, the outgoing wave, and dropping the time dependent terms,

$$\zeta_{i,j} + u_{i,j}h/c = A(1+\Delta^2)\,. \tag{4}$$

This equation was used to replace the open boundary condition in the model described by Webb (2013). The interior velocity points are treated as before but a velocity component such as $u_{i,j}$ in fig. 1 does depend via the Coriolis terms on the values of $v_{i,j}$ and $v_{i,j-1}$.

Equation 4 does not specify the tangential velocity v on the open boundary but setting the values to zero would introduce strong shears, which would be unrealistic. The values are therefore set equal to v on the first interior row, i.e. $v_{i,j}$ is set equal to $v_{i+1,j}$.

3 The Response Function

The present study uses the same configuration of model grid, coastline, depths and bottom friction coefficient as Webb (2013). The only change is in the open boundary condition, which now has a unit amplitude incoming wave everywhere on the boundary and an outgoing wave determined by the model.

The analysis makes use of the response function $R(\omega)$, which is defined at each point of the model by the equation,

$$R(\omega) = \zeta(\omega)/\zeta_i\,, \tag{5}$$

where $\zeta(\omega)$ is the amplitude of the resulting wave at point $\boldsymbol{x}$ and ζ_i is the amplitude of the incoming wave. As discussed in previous papers, for linear systems $R(\omega)$ is an analytic function of ω with poles at the angular velocity of each resonance of the system. It is applicable to tides because over most of the ocean non-linear effects are small, and so to a first approximation tides can be treated as a purely linear system.

Figure 2 shows the amplitude of the resulting response function, between zero and 30 rad/day (radians per day), for the ports of Portishead, St. Malo, Workington and Le Havre. These are the same ports as studied in Webb (2013) and so allow a comparison to be made between the response to the Dirichlet boundary condition, used there, and the present mixed boundary condition.

One difference between the two boundary conditions is that the response at zero angular velocity now has a value of two whereas previously it had been one. The difference

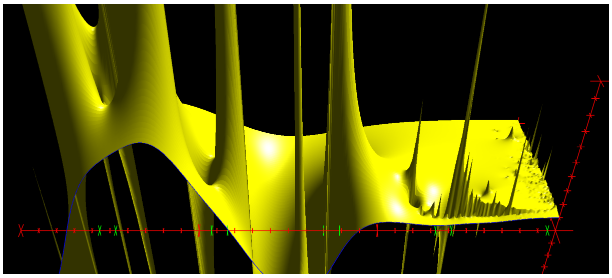

Portishead

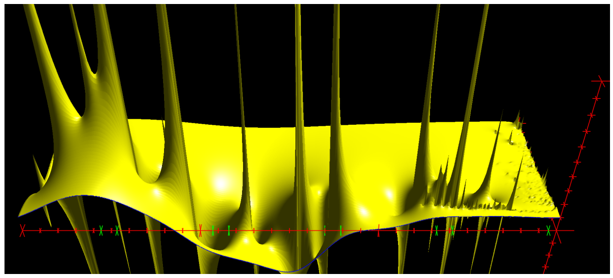

St. Malo

Fig. 3. The real components of the response function plotted as a function of complex angular velocity at Portishead and St Malo. The origin (0,0) is on the right with the positive real axis (in red) running from right to left and the negative imaginary axis running into the figure. Function values on the real axis are plotted in blue. The horizontal axes have red crosses every 1 $\mathrm{radian/day}$. The vertical axis has been scaled to match the equivalent figures in Webb (2013) with crosses now at intervals of two. On the real axis green crosses indicate the limits of the tidal bands near 1 (diurnal), 2 (semi-diurnal), 3 and 4 cycles per day.

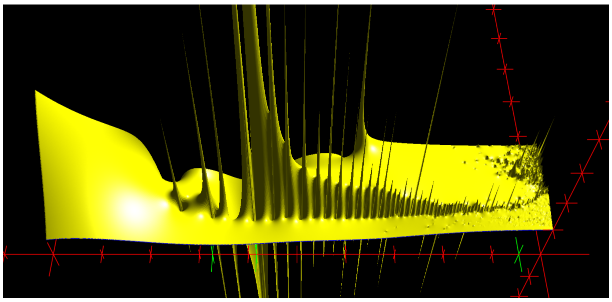

Fig. 4. An expanded view near the origin of the real component of the response function at Portishead.

arises because, in the present case, the incoming and outgoing both have unit amplitude and zero phase at zero angular velocity.

As the angular velocity increases the general pattern of the response functions amplitude is similar to that of the original paper. However, in the present case, the peaks are less pronounced and, especially above 10 rad/day, the amplitudes are less than twice the value obtained previously with Dirichlet boundary conditions. The amplitude ratio varies with angular velocity but at 12 rad/day at Portishead the ratio is 1.66, at St Malo it is 1.67 and at both Workington and Le Havre it is 1.93.

3.1 The Complex Response Function

An important advantage of the model is that it can be run with complex values of angular velocity and so allows an investigation of the analytic form of the response function. Two sets of runs were carried out. The first covered the complex angular velocity plane between the origin and the points (0 -i10), (30 -i10) and (30 +i0) radians per day at intervals of 0.1 rad/day. Figure 3 shows the resulting real component of the response function for the Portishead and St Malo.

Comparison between the present results using a radiational boundary condition and Webb (2013) which used a fixed (Dirichlet) boundary condition shows that there are differences but that most are small. Thus, above 10 rad/day, the positions and thicknesses of the poles associated with the main gravity wave resonances appear to have changed only by small amounts. The resulting change in the response at real values of angular velocity is also small.

For the semi-diurnal tides, the two most important resonances are the two near 13 and 15 rad/day. At St. Malo the poles have about equal residues, as they did with the Dirichlet boundary condition. At Portishead the lower angular velocity resonance is still the strongest, but the second now appears to be slightly more significant.

There are greater changes at low values of angular velocity and these were investigated in a second run which covered the regions between the origin and the points (0 -i3), (10 -i3) and 10 rad/day at intervals of 0.02 rad/day. Figure 3 shows the resulting real part of the response function at Portishead.

It still shows the main 'wall' of resonances at low angular velocities and shows that the strongest resonances still have real values of angular velocity near 6 rad/day. However two additional lines of resonances, one nearer the real axis and one with approximately twice the imaginary component, are no longer present. Also the main line of resonances stops near 7.5 rad/day whereas before it extended beyond 9 rad/day.

3.2 Resonance Angular Velocities

Resonance angular velocities were found using the method developed in Webb (2012). This fits the response function in the neighbourhood of each resonance pole with the function,

$$R(\omega) = R_j/(\omega - \omega_j) + A + B\omega. \tag{6}$$

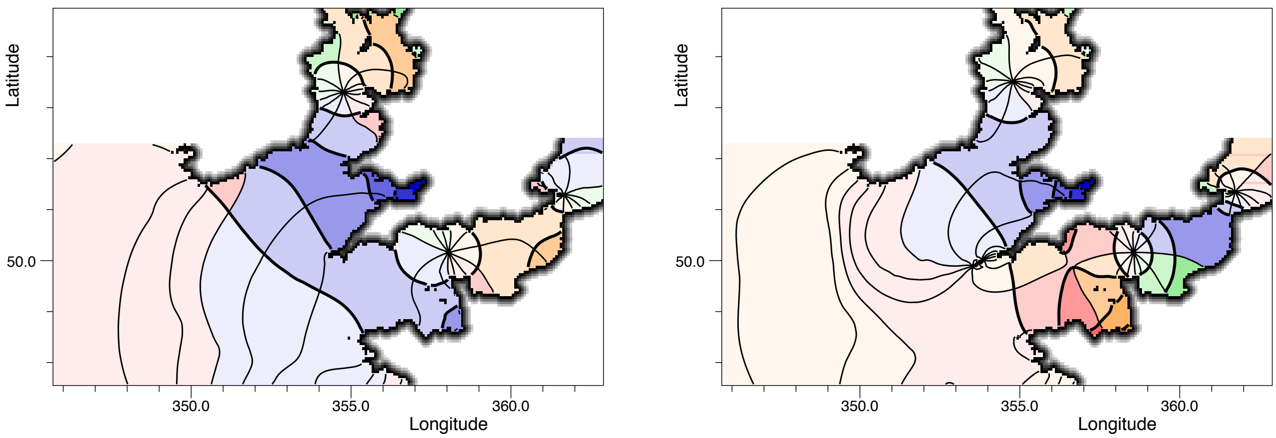

Resonance ‘D’ Resonance ‘E’

Fig. 5. Amplitude and phase of the resonances ’D’ and ’E’ (table 1). The resonance is normalised such that its maximum amplitude is 1.0. Colours denote phase (blue , 180°-270°; green, 270°-360°; orange, 0°-90°; red, 90°-180°) with additional thin contours plotted at intervals of 30°. Colour intensity denotes amplitude. The lightest colours, seen near the shelf edge and beyond denote amplitudes less that 1% of the maximum. The remaining bands separated by thick contours denote 1%-20%, 20%-40%, 40%-60%, 60%-80% and 80%-100% of the maximum.

Table 1. Real and imaginary components of angular velocity (in radians per day) for the main resonances.

	No Radiation Angular velocity		With Radiation Angular velocity	
	Real	Imag.	Real	Imag.
A	3.9057	-2.0017	3.7677	-1.9734
Ba	5.3612	-0.7935	5.1932	-0.6832
Bb	5.5931	-0.8501	5.4550	-0.7504
Bc	5.7544	-0.8720	5.7883	-1.0207
Bd	5.9688	-0.9047	5.9080	-0.8623
Be	6.2037	-0.8680	6.4459	-0.8901
Bf	6.5763	-0.8760	6.7886	-0.9250
C	8.2549	-1.8567	7.8938	-2.2269
D	13.1387	-1.6323	12.7094	-2.0774
E	14.6609	-2.0767	14.5130	-2.1991
F	17.4442	-3.1087	17.4536	-3.2013
G	21.0201	-2.2989	20.8443	-2.7435
H	22.0992	-3.3991	22.0546	-3.4135
I	24.2709	-2.9582	23.9297	-3.3606
J	25.5625	-3.1394	25.5524	-3.1610
K	27.8690	-2.9693	27.8511	-3.4583

where ω_j is the angular velocity of resonance j and R_j is its residue. The constants A and B represent the smooth background due to distant poles. The method used was an iterative one which made use of the values of R calculated for four points forming a cross at a distance of 0.02 rad/day from the previously calculated resonance position.

The results for the gravity wave resonances and continental shelf resonances nearest those discussed in Webb (2013), are given in table 1. In most cases, the change to the present radiation boundary condition reduces the real component of angular velocity by a small amount. The exceptions are resonance ’F’ and some of the ’B’ resonances. Webb (2013) showed that that the latter resonances involved the coupling of one gravity wave resonance with a series of continental shelf waves.

The table also shows that most cases the imaginary component becomes more negative, the exceptions being resonance ’A’ and some of the ’B’ resonances. The change is much less than that found by Webb (2011) for a one-dimensional channel in which the imaginary components doubled.

3.3 Resonance Structure

Figure 5 shows the spatial structure of the two primary resonances affecting the Bristol Channel and Gulf of St Malo. These results using a radiational boundary condition can be directly compared with the corresponding figure of Webb (2013).

On the shelf seas, the amplitude and phases of resonance ’D’ are modified only slightly by the change in boundary conditions. With a radiational open boundary the maximum amplitude is still at the head of the Bristol Channel and there is again a much smaller second maxima in the Gulf of St Malo. The relative amplitudes between St Malo and Portishead has dropped slightly from 0.24 to 0.23 and the relative phase is reduced from 63°to 40°.

With both boundary conditions the mode shows anticlockwise amphridromes in the centre of the English Channel between Southampton and Cherbourg and in the centre of the Irish Sea between Dublin and Holyhead. Although

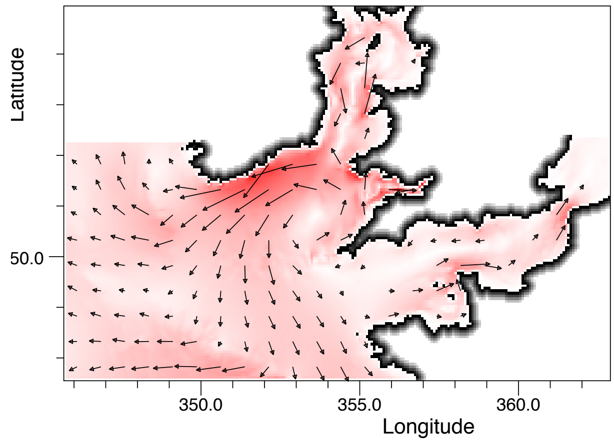

Fig. 6. Energy flux vectors for resonance 'D'.

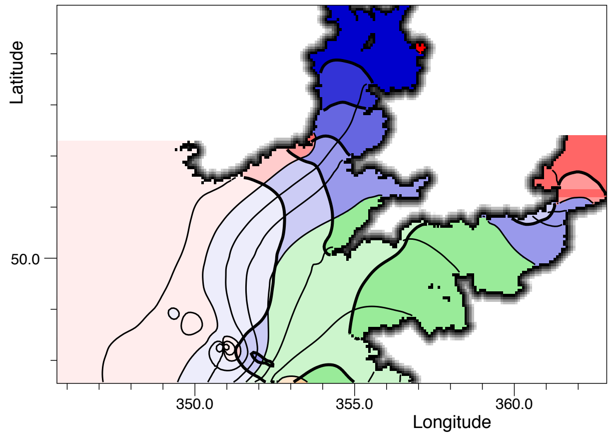

Fig. 7. Amplitude and phase of resonance 'Bc'. Contours and colours as in fig. 5.

there is no amphridrome there, plots of the energy flux vectors show an anti-clockwise circulation in the south-western approaches which feeds one branch into the English Channel, along the French coast, a second feeding into the Bristol Channel and a third northwards along the Welsh coast.

With the radiational boundary condition there is an additional flow of energy through the southern boundary on the continental shelf, a northward flow in the deep water to the west of Ireland and a westward flow near the western limit of the Porcupine Sea Bight. In the latter case the wave has some similarity to a Kelvin wave propagating out of the model domain with shallower topography to the right. The southward flow of energy out of the model on the shelf, is not in the form of a Kelvin wave. There is a broad amplitude maxima in the centre of the shelf with phases increasing towards the south-east.

The properties of resonance 'E' are generally similar. The main change is that, with the radiational boundary condition, the region of maximum amplitude moves from the south-east corner of Gulf of St. Malo to the head of the Bristol Channel. As a result the relative amplitudes of St. Malo and Portishead are reduced from 0.88 to 0.56. In contrast the relative phases stay remarkably constant, being 251°with the original boundary condition and 252°with the radiational boundary condition.

Compared with resonance 'D', the plots of energy fluxes in the English Channel and Irish Sea are more symmetric with much larger flows back towards the Celtic Sea. At the same time the fluxes within the Celtic Sea itself are relatively smaller. With the open boundary condition energy is still lost to the south, on the continental shelf. Energy is also lost to the west and north as with resonance 'D' but the relative amplitude is much smaller.

3.3.1 Resonance Bc

Figure 7 shows the structure of resonance 'Bc'. Comparison with Webb (2013) shows that the use of the radiational boundary condition has reduced the continental shelf wave component by a large amount. This time no scaling has been required and figure shows that the resonance is primarily a standing wave with maximum amplitude at the northern end of the Irish Sea but that there is some coupling with a standing wave of the English Channel. The radiational boundary condition similarly reduced the continental shelf wave component of all the other 'B' resonances.

3.4 Resonance Contributions to the Response Function

Once the resonance angular velocities and residues are known, it is of interest to calculate the contribution of each resonance to to the response of the ocean at real values of angular velocity. As the contribution of distant resonances varies only slowly with angular velocity, over a limited region of angular velocity the response function can be expanded in the form:

$$R(x,\omega) = \sum_j R_j(x)/(\omega-\omega_j) + S(x,\omega) + B(x,\omega), \tag{7}$$

where the sum j is over key nearby resonances. $R_j(x)$ is then the residue at position x and w_j, is the resonance angular velocity. The symmetry term $S(x,\omega)$, is not essential but it is easy to calculate and represents the contribution from the conjugate set of poles. $B(x,\omega)$ is the smooth background due to distant poles.

Figure 8 shows the key resonances contributing to the response function between 11 and 14 rad/day at Portishead and St Malo. The key resonances are the same as in Webb (2013) and, except for a small change in phase, their roles are similar. Thus at Portishead the main contribution, in terms of

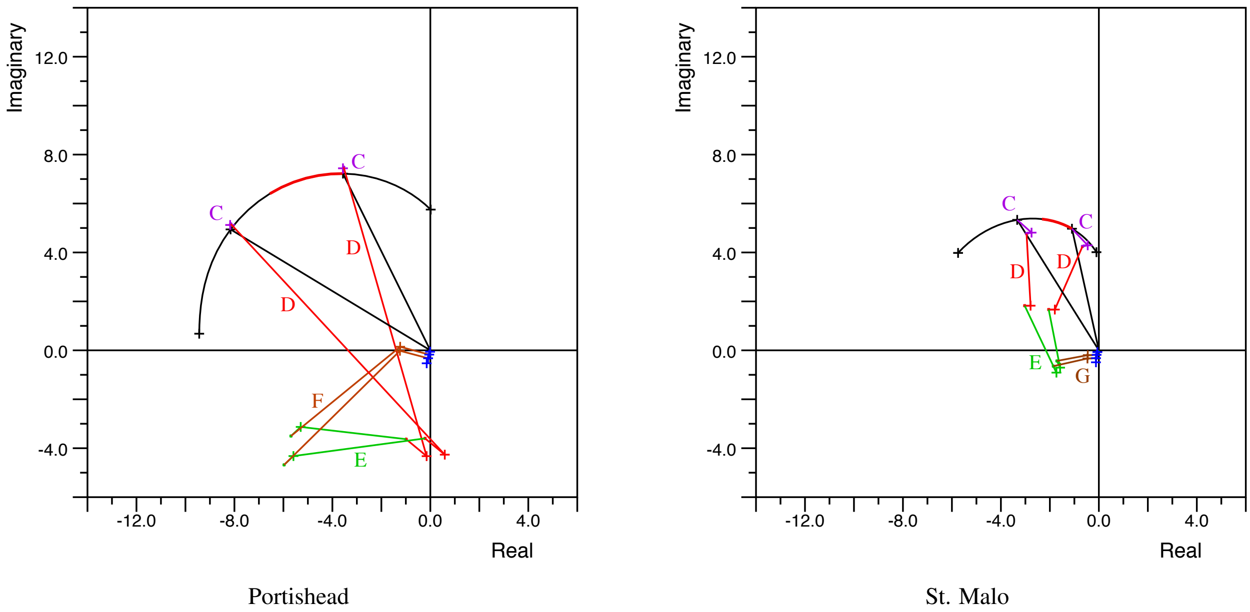

Fig. 8. Polar plot of the Portishead and St Malo response functions (black) between 11 and 14 rad/day. Crosses are at intervals of one radian per day. The figure also shows the contributions at 12 and 13 rad/day of resonances C (purple), D (red), E (green), F (brown) and G (dark brown) of table 1, their much smaller conjugates (same colours) and the residual (blue).

both amplitude and phase change, comes from resonance 'D'. Resonances 'E' and 'F' have roughly equal amplitudes, but 'E' is more than 90°out of phase with 'D' and so has the effect of reducing the response at Portishead.

At St Malo the contribution from resonance 'D' is much smaller, so 'D' and 'E' now have roughly equal amplitudes. They also have roughly equal phase so together they generate a much greater amplitude response than they would by themselves.

4 Conclusions

The present study has shown that the effect of the radiational boundary condition on the resonance angular velocities is much less than was expected from a study of a one-dimensional system (Webb, 2011). However, as expected from that study, both the real and imaginary components become more negative with the imaginary components changing most.

The spatial structure of each resonance is also changed but, for the gravity wave resonances, the changes are small. Each resonance now has an small outgoing wave at the open boundary and, as shown in fig. 8, there is a phase change in each resonances' contribution to the response function. There are only small changes in the relative phases and amplitudes and as a result there appears to be no really significant change to the physical processes affecting the main semi-diurnal tides.

The Rossby wave resonances are affected by the changed boundary condition in that the large continental shelf wave component is greatly reduced. However the net effect of the diurnal tide in the English Channel and Irish Sea is small.

The large continental shelf wave components in Webb (2013) may have been an artifact of the Dirichlet boundary condition. Using a long gravity wave radiation condition, as has been done here, reduces the effect but it may be that a boundary condition tuned to the properties of shelf waves is needed in the regions of the continental slope and shelf.

4.1 The Radiation Condition

Overall the study has the surprising conclusion that the effect of adding a radiational boundary condition is small. Thus one might ask, if it is so difficult for resonance energy to be lost to the deep ocean, why does it appear to be so easy, in reality, for tidal energy to cross from the deep ocean into the shelf seas?

For the moment the most likely answer is that it is the radiational boundary condition that is a fault. To work correctly this needs to allow all waves to propagate outwards without reflection. The Flather (1976) scheme does this for gravity waves propagating normal to the boundary but if a wave is propagating at an angle, the relationship between height and normal velocity will be wrong and part of the energy will be reflected.

The boundary condition also does not take into account the Coriolis term, so any Poincaré waves (LeBlond and Mysak,

1978) arriving at the boundary will be reflected. Kelvin waves in a flat bottomed ocean and propagating normal to the boundary should pass through but if there is any continental slope its phase speed will depend on the overall depth profile and not on the local depth (LeBlond and Mysak, 1978; Huthnance, 1975). The mismatch in phase speeds will again reflect energy at the open boundary.

The problem needs further research. One option would he to extend the model region to the north and south in the deep ocean. This should be done far enough to the north that an well defined outgoing Kelvin wave can be formed and identified. It also should exted far enough to the south that most of any southward energy flux on the shelf, as seen in resonance 'D', has a chance to decay away due to bottom friction.

References

Flather, R. A.: A Tidal Model of the North-west European Continental Shelf, Mmoires Socit Royale des Sciences de Lige, 10, 141–164, 1976.

Huthnance, J. M.: On Trapped Waves over a Continental Shelf, Journal of Fluid Mechanics, 69, 689–704, 1975.

LeBlond, P. and Mysak, L.: Waves in the Ocean, Elsevier, 1978.

Webb, D. J.: Notes on a 1-D Model of Continental Shelf Resonances, Research and Consultancy Report 85, National Oceanography Centre, Southampton, http://eprints.soton.ac.uk/171197, 2011.

Webb, D. J.: On the Shelf Resonances of the Gulf of Carpentaria and the Arafura Sea, Ocean Science, 8, 733–750, 2012.

Webb, D. J.: On the Shelf Resonances of the English Channel and Irish Sea, Ocean Science Discussions, 10, 393–433, doi:10.5194/osd-10-393-2013, 2013.